PCCP

Preparation, characterization and applications of free-standing single walled carbon nanotube thin films

Frank Hennrich,[a] **Sergei Lebedkin,**[b] **Sharali Malik,**[a] **Joseph Tracy,**†[a] **Matthias Barczewski,**[a] **Harald Rösner**[a] **and Manfred Kappes**[ab]

[a] *Forschungszentrum Karlsruhe, Institut für Nanotechnologie, Postfach 3640, 76021 Karlsruhe, Germany*
[b] *Universität Karlsruhe, Institut für Physikalische Chemie, Kaiserstr. 12, 76128 Karlsruhe, Germany*

A method for the reliable fabrication of less than 200 nm thick, free-standing purified-SWNT films having large surface areas exceeding several cm^2 is described. Films were characterized using a variety of optical, microscopic and spectroscopic methods. The procedure was also used to prepare thin films of as-prepared, acid-cut and octadecylamine (ODA) functionalized SWNTs. Such samples allow facile transmission measurements of SWNT derived solids.

1.   Introduction

Since their discovery, multiwalled carbon nanotubes (MWNTs)[1] and single-wall carbon nanotubes (SWNTs)[2,3] have attracted great interest because of their unique mechanical and electronic properties.[4–8] SWNTs are composed of single (capped) graphene cylinders, with typical diameters of 1–2 nm although larger diameters of up to nearly 6 nm may be accessed depending on production method and catalyst.[9] SWNT bulk samples are often made up of intertwined crystalline "bundles", which in turn consist of hexagonally close-packed individual tubes. Bundles form during SWNT synthesis.[10]

   Among known production methods, the laser ablation procedure pioneered by the Smalley group produces the highest quality SWNT material in terms of yield relative to carbon "feed" and resulting tube defect densities.[11] For example, laser ablation of a graphite target containing a "standard" Ni/Co catalyst in a 1200 °C flowing argon atmosphere generates tubes having a characteristically narrow diameter distribution between about 1.2–1.4 nm. Depending on other production parameters as well as post-production chemical processing of the resulting material, close-packed bundles of diameter ranging from ∼2 to ∼100 nm are observed.[12] Bundle lengths of >2 μm are common. Thick (a few tenths of a mm), free-standing films of this material, so-called "buckypapers",[13] can be made by filtration from suspension at various stages of purification and are available commercially in large continuous mats having >1 cm^2 surface areas.

   Thinner free-standing buckypapers hold promise for transmission studies in various applications ranging from impurity analysis by electron microscopy, through optical probes of the tubes themselves, to spectroscopic measurements of SWNT "surface" chemistry. However, in spite of extensive probes of large scale (oriented) MWNT films ranging in thickness down to sub 500 nm,[14] thin SWNT films are practically uncharted. Exceptions are: (i) transmission EELS probes of small pieces of nominally 100 nm thick films supported on cop-per microscope grids having 0.1 × 0.1 mm openings[15] and (ii) studies of thin ribbons composed of magnetically oriented SWNT bundles.[16] In particular, while it is known that individual SWNTs have high tensile strengths, there have as of yet been no attempts to test the inherent lower limit to the thickness of large area free-standing SWNT films under ambient conditions. Here, we report that 1 × 1 cm uniform free-standing films of significantly less than 200 nm thickness may be produced and readily handled. This is possible not only for purified SWNTs, but also for acid-shortened SWNTs as well as for chemically functionalized SWNTs.

2.   Experimental procedure

2.1   Synthesis and workup of SWNTs

The SWNTs were made by the laser ablation technique[2,3] using a 1 : 1 Ni/Co catalyst (1 at.% each). Details of our set-up have been described in a previous publication.[9] As prepared tubes (SWNTs (**I**)) were subjected to purification as follows. First the raw soot was refluxed with 2–3 M HNO_3 for 48 h. After this, the whole reaction mixture was ultracentrifuged at 20 000 *g* in order to subsequently remove the remaining acid solution by decanting. The solid residue was then resuspended in water containing 0.2 wt.% of the surfactant Triton X-100 (Roth). The concentration of SWNTs was chosen to be about 0.3 mg ml^{-1}. To remove the small particles, this suspension was run over/through (and flushed with additional Triton X-100 solution) a home-built ultrafiltration cell using 0.2 μm pore sized membrane filters (Schleicher&Schuell; cellulose nitrate, 90 mm ∅ (**A**)). This procedure generates SWNTs (**II**) of approx. 99% purity by weight as determined by oxidative thermogravimetric analysis (TGA). The impurities are mainly large nanocrystallites of a 1 : 1 alloy of Co and Ni encapsulated by several turbostratic carbon layers as observed in transmission electron microscopy (TEM). Methods to obtain higher-purity (>99.9%) SWNTs are currently under investigation in our laboratory and will be reported in more detail together with a further description of the Co/Ni nanocrystallites and their properties.[17]

---

† Present address: Department of Chemistry, Massachusetts Institute of Technology, Cambridge, MA 02139, USA.

2.2 ODA derivatization

Smalley *et al.* have shown that SWNTs can be cut into pieces several 100 nm long by treating them with concentrated acids.[18] Haddon *et al.* subsequently succeeded in derivatizing cut SWNTs with octadecylamine (ODA) by making use of the fact that the SWNTs possess a high concentration of carboxylic acid functional groups after cutting.[19] The carboxylic acid groups are first converted into acylchloride groups by treatment with thionyl chloride. The acid chloride-functionalized SWNTs are then susceptible to reaction with amines to give amides. In a recent publication, Haddon *et al.* have shown by means of IR-spectroscopy that 4–8% of the SWNT carbons may be functionalized by ODA in this fashion.[20] It has also recently been reported that cut SWNTs may be directly reacted with ODA to make non-covalently linked zwitterionic species in high yield.[21]

As part of this study we have followed a third synthetic approach, which we believe generates amide linked ODA-SWNT derivatives as in ref. 19, but in fewer steps. In peptide synthesis, dicyclohexylcarbodiimide (DCC) is used as an efficient dehydrating agent.[22] Analogously, using DCC allows a direct coupling of ODA and the SWNT carboxylic functions by elimination of water under mild, neutral conditions.

For this, a water suspension + Triton X-100 of purified SWNTs is first concentrated to about 3 mg ml^{-1} by simply heating to boiling. The residue is vacuum filtered through a membrane filter with 0.4 μm sized pores (Schleicher&Schuell; regenerated cellulose, 47 mm $\varnothing$ (**B**)) to get buckypaper. A piece of buckypaper weighing 100 mg is then treated with 40 ml of a 1 : 3 mixture of conc. HNO$_3$ (65 wt.%, Sigma-Aldrich) and H$_2$SO$_4$ (95–98 wt.%, Sigma-Aldrich) for 4 h in an ultrasonic bath (Bandelin, 480 W). After acid treatment, the reaction mixture is diluted with deionised water to about 400 ml, again filtered over 0.2 μm pore sized membrane filters (Schleicher&Schuell; regenerated cellulose, 47 mm $\varnothing$ (**C**)), washed with several ml of acetone and dried in vacuum for about 12 h to yield "conc. acid cut SWNTs" = SWNT (**III**). We observe the loss of about 50% of the starting material during the acid treatment.

For the ODA derivatization, 100 mg of dried, cut SWNTs (**III**), 270 mg ODA and 210 mg DCC were added to dry DMF and stirred under Ar for 24 h. After the reaction, the reaction mixture was filtered off over 0.2 μm pore size membrane filters (**C**), washed with ethanol and acetone and dried in vacuum for 12 h. In contrast to solid SWNT (**I**), SWNT (**II**) and SWNT (**III**) samples, the ODA derivatized SWNTs (**IV**) turn out to be rather soluble in *ortho*-dichlorobenzene (ODCB (~1 mg ml^{-1})). Such suspensions are stable over at least several months under ambient conditions and may again be filtered to form (fully redissolvable) films. From ^{1}H NMR measurements on these ODCB suspensions, we estimate that 4% of the SWNT (**IV**) carbons are functionalized.[23] Absorption measurements on thin films of **IV** provide further evidence for an ODA loading of this magnitude, as discussed in section 3.4. It is presently not clear as to what degree bundle uniformity is modified by ODA derivatization (*e.g.* enrichment of ODA linkages in the outermost, most highly etched tubes).

2.3 Preparation of SWNT thin films

Thin films of **II** were prepared by vacuum filtration of SWNT suspensions in water/Triton X-100 using 0.2 μm pore size membrane filters (Schleicher&Schuell; cellulose nitrate, 47 mm $\varnothing$ (**D**)). Low suspension concentrations (on the order of 6–18 μg ml^{-1}) were necessary to obtain high quality films. For this, we appropriately diluted our SWNT stock suspensions with deionised water. To make films of **I**, **III** and **IV** we used SWNT suspensions diluted in DMF again to concentrations of about 6–18 μg ml^{-1}. Here, stability to solvent required use of 0.2 μm pore size membrane filters composed of regenerated cellulose (**C**). The as-prepared SWNTs (**I**) were suspended by treating them for 30 min. in an ultrasonication bath and subsequently centrifuged at 5000 g to partially remove catalyst particles and amorphous carbon by decanting. Typically, approximately 50 ml of dilute suspensions were processed over the filter assembly. Subsequent to filtration, nanotube films were repeatedly washed with several ml of water or acetone (again with vacuum applied). Finally, the nanotube film and filter were transferred to a vacuum chamber and evacuated for 30 min to a final pressure of 10^{-3} mbar at room temperature.

Thereupon, films were removed from the filter using adhesive tape (Tesa) selectively applied to the top surface. Before fastening to the nanotube film surface, an approx. 2 cm^2 rectangular opening was cut in the adhesive tape. The mechanical stability of even the thinnest nanotube films (see below) then allowed for essentially hole and tear-free removal of the corresponding free-standing area by careful peeling. The free-standing films were then affixed to a metal frame and further dried in high vacuum (10^{-6} mbar) for 12 h at room temperature before subsequent analysis. Fig. 1 shows a photographic image of a 300 nm film of **II** thin enough to transmit visible light.

2.4 Instrumental analysis tools

Films were probed by a variety of methods. Optical and electron microscopy were used to establish film morphology, film thickness, hole density and hole size distribution. Specifically we made use of (in order of increasing spatial resolution): visible light microscopy (Leica DMLM), confocal visible light microscopy (Leica TCS SP2-X1 confocal microscope, 514 nm laser wavelength; *ca.* 300 nm lateral resolution), scanning electron microscopy (LEO 1530 SEM; <10 nm lateral resolution), atomic force microscopy (Digital Instruments Multimode with Nanoscope 3 converter AFM; <1 nm lateral resolution) and transmission electron microscopy (TEM, Philips CM 30 ST TEM; 0.2 nm lateral resolution). SEM and TEM specimens were cut with a scalpel from samples of the free standing SWNT thin films.

The film thicknesses were obtained using an AFM in tapping mode by measuring the height difference at the film edge between the film surface and an underlying substrate. For the AFM and confocal microscope sample preparation, small cut squares (*ca.* 5 × 5 mm) of SWNT films were floated on the
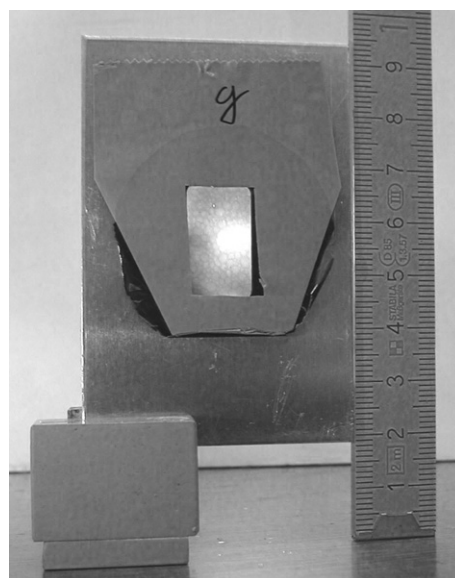
Fig. 1 Photograph of a 300 nm thick free-standing SWNT (**II**) film (approx. 2 cm^2) mounted on a metal frame (back-illumination).

surface of deionised water in a Petri dish. A square (*ca.* 10×10 mm) of Si wafer (CrysTec, Kristalltechnologie; thermally oxidised (600nm) polished) substrate was then brought up from under the film sample. The so deposited SWNT film was allowed to air dry and was then examined under the light microscope to ensure that the film sample was lying flat on the Si substrate.

Films were also probed by UV–VIS–NIR absorption spectroscopy (Cary 5E, Varian; 200–3300 nm spectral range; 1 nm spectral resolution) and FT-IR (IFS-28, Bruker; 2 cm^{-1} spectral resolution, 100 scans).

3. Results and discussion

3.1 Surface uniformity from large to small length scales

Among the materials prepared, only films of **II** were extensively probed with regard to film uniformity and thickness. Optical microscopy and SEM of film surfaces with thickness greater than about 300 nm indicated high sample uniformities with typically <3% of the overall surface composed of resolvable holes, cracks or impurities down to 2 μm length scale.

SEM investigations were carried out on a number of SWNT (**II**) thin films. Both sides exhibit the typical interwoven nanotube bundles known from previous studies of clean buckypaper samples. In addition, small particulates (see below) were also observed. Images obtained at a variety of SEM focal planes indicated that on a sub-micron length scale the front surface, corresponding to the side facing the suspension before filtering, was significantly smoother than the back (see Figs. 2(a) and (b)). A view of a curved specimen looking from the side (see Fig. 2(c)) shows this effect most clearly: the front surface comprises tube bundles with their long axes mostly lying roughly in the plane of the film, while the back shows a significant number of SWNT bundles to be standing out of the film—likely as a result of peeling from the membrane filter pore structure.

TEM measurements of **II** were performed at film edges and at the edges of mechanically punched holes. This was necessary because 200 nm SWNT films (see section 3.2 below) are still too thick to allow sufficient electron transmission. We typically observed individual tubes within bundles with diameter distributions similar to those that have been reported previously. In addition, metal nanoparticles enclosed in turbostratic carbon shells were often seen.[12] Metal particle sizes (roughly spherical) were typically on the order of 6–30 nm with carbon shells typically adding another ∼5 nm to the diameters. Details will be reported in a future study.[24]

3.2 Film thickness and thickness uniformity

From AFM film thickness measurements for films deposited onto silicon, we inferred that the thinnest large area (>1 cm^2) free-standing films, which could be reproducibly generated and handled under ambient conditions, were of the order of 200 nm (average thickness with typical local thickness variations corresponding to one or two bundle diameters).

Fabrication of films thinner than 200 nm is primarily limited by the corrugation and pore structure of the membrane filters used. Local vertical excursions in the filter material become comparable to overall SWNT film thickness, which results in direct mechanical contact between adhesive tape and membrane filter. If this problem could be eliminated, for example, by going to flatter metal oxide or ion track membrane filters, large area sub-100 nm thickness free-standing films appear realizable—in the sense that they would not tear under their own weight when horizontally supported by a 1 cm × 1 cm frame under ambient conditions.

3.3 Density and packing

Average SWNT (**II**) film densities were determined from AFM derived film thicknesses together with the volumes of SWNT stock suspension used to prepare the films and the mass density of SWNTs in the suspension. Over the film thickness range studied (200–600 nm) we observed an average density of 1.2 ± 0.1 g cm^{-3}, which is lower than graphite-HOPG (2.26 g cm^{-3})[25] or C_{60} (1.72 g cm^{-3})[25] but significantly larger than that which is obtained in typical "bulk" buckypapers having several tenths of a millimetre thickness (0.6 g cm^{-3}). By comparison, the density of an "infinite" hexagonally close-packed bundle of (10,10)-SWNTs having diameter of 1.3 nm and nearest center-to-center distances of 1.65 nm is 1.17 g cm^{-3}. Thin film density is likely primarily a function of solvent flow during filtering and in this sense is not an intrinsic property of the material. There was no systematic decrease in average density with increasing film thickness over the thickness range (up to 600 nm) probed.

3.4 Spectroscopy

Fig. 3 shows a series of UV–VIS–NIR absorption spectra obtained for SWNT (**II**) films of various thicknesses under ambient conditions. We have assumed that to first order, measured extinction may be equated to absorption (*i.e.* that light scattering contributions are negligible). Plotted in the inset are the corresponding absorption values at 5 eV *versus* filtered SWNT mass. Note the linear dependence and that we observed no photochemical change as evidence by absorbance changes under the experimental conditions (light intensities) used. From the data of Fig. 3, we obtain an absolute absorption cross section of $2.9 \pm 0.7 \times 10^{-18}$ cm^2 atom^{-1} at 5 eV. This compares to the value of 5.85×10^{-19} cm^2 atom^{-1} for C_{60} at the same energy.

Analogous measurements were also carried out for ODA derivatized films (**IV**). ODA does not absorb significantly at 5 eV. Under the assumption that the 5 eV absorption cross section (per SWNT C-atom) of ODA derivatized films is not significantly changed relative to purified SWNT (**II**) samples, we estimate that approximately 5% of SWNT carbon atoms in **IV** have ODA molecules attached to or associated with them.
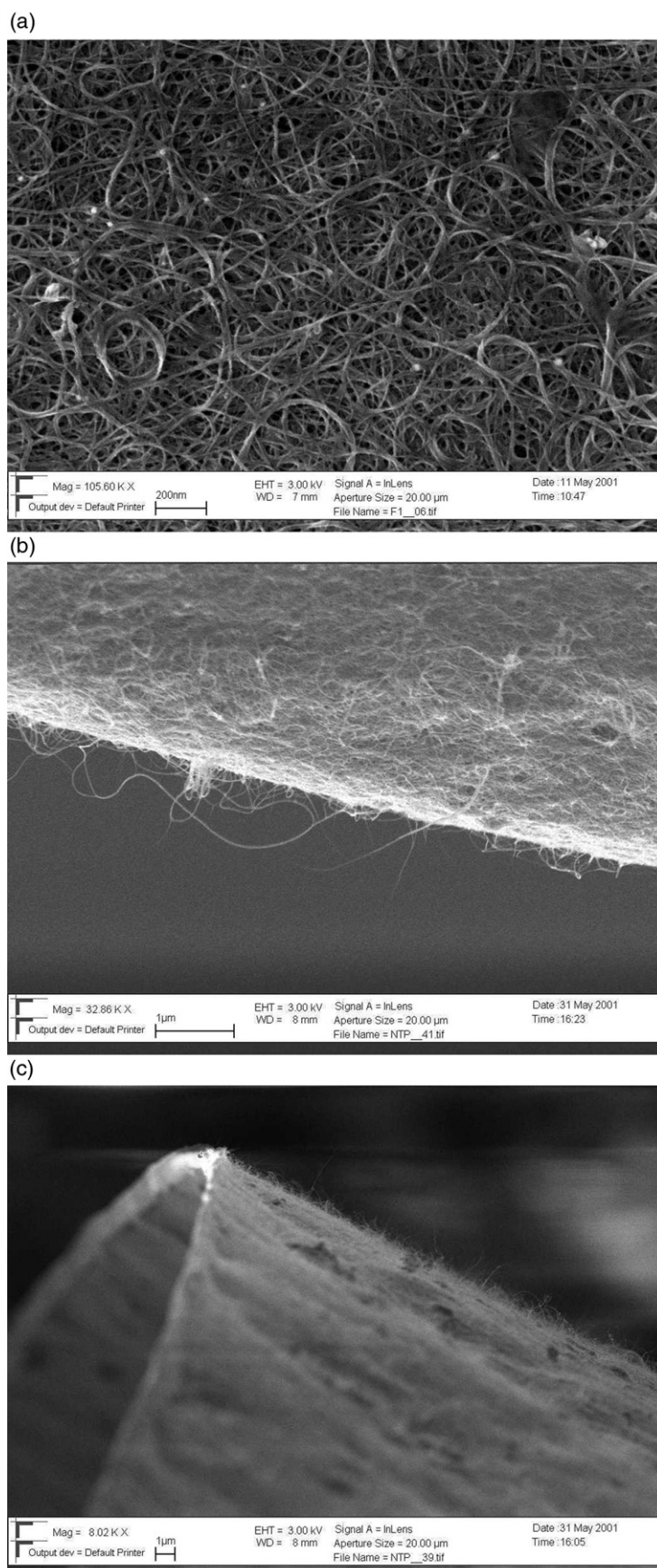
Fig. 4 contains FT-IR transmission measurements of as-prepared (**I**) and ODA derivatized (**IV**) SWNT films of roughly 300 nm thickness—again under ambient conditions. Shown in the insert are background subtracted data. The ODA derivatization is apparent in the spectrum obtained for **IV** from prominent signals at 2850, 2920 and 2956 cm^{-1} due to (–C–H)-stretch modes of the alkyl chain. The IR transmission spectrum of the as-prepared SWNTs (**I**) contains no features. The purified SWNTs (**II**) show features in the region between 1500 and 1800 cm^{-1}, which are most likely due to defects created during the diluted nitric acid purification step—spectrum not shown here. In this acid treatment up to 5% of the carbon atoms are probably oxidized to –COH, –C=O or even –COOH.[26,27] A more detailed study will be published elsewhere.[24]

Summary

We have shown that it is possible to easily prepare large area free-standing thin films (<200 nm) of as-prepared, purified and derivatized single-walled carbon nanotubes. These films may in turn be readily adsorbed onto flat surfaces such as glass or silicon.

The large area thin films provide a novel sample configuration for physical characterization of SWNT bulk samples and may be conveniently used in a variety of applications, notably large area transmission measurements under controlled atmosphere and temperature (*e.g.* frequency or time domain

(a)

Mag = 105.60 K X   200nm   EHT = 3.00 kV   Signal A = InLens   Date :11 May 2001
Output dev = Default Printer   WD = 7 mm   Aperture Size = 20.00 μm   Time :10:47
    File Name = F1__06.tif

(b)

Mag = 32.86 K X   1μm   EHT = 3.00 kV   Signal A = InLens   Date :31 May 2001
Output dev = Default Printer   WD = 8 mm   Aperture Size = 20.00 μm   Time :16:23
    File Name = NTP__41.tif

(c)

Mag = 8.02 K X   1μm   EHT = 3.00 kV   Signal A = InLens   Date :31 May 2001
Output dev = Default Printer   WD = 8 mm   Aperture Size = 20.00 μm   Time :16:05
    File Name = NTP__39.tif

Fig. 2 SEM images of SWNT (**II**) films: (a) front surface (suspension side), (b) back surface (filter side) and (c) cross sectional view.
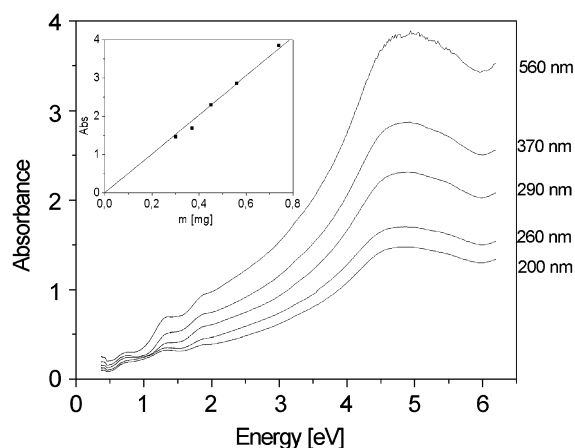
Fig. 3 UV–VIS–NIR absorption spectra of SWNT (**II**) films of various thicknesses. The inset shows absorption at 5 eV as a function of the mass of filtered tubes in each film.
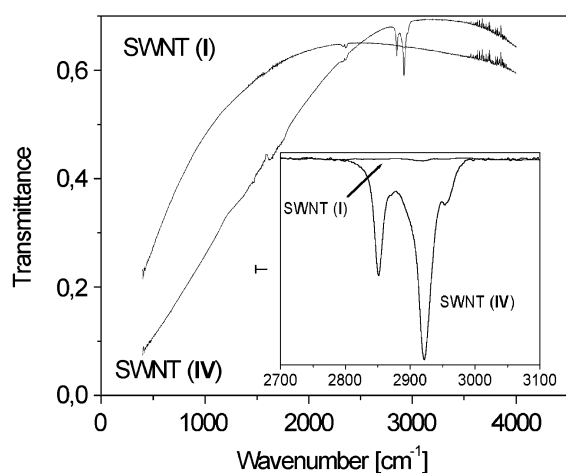
Fig. 4 FT-IR transmission measurements obtained for (a) an as-prepared SWNT (**I**) film and (b) a film resulting from ODA derivatized nanotubes (**IV**)—both about 300 nm thick. Insert shows background subtracted (–CH)-stretch region.

electronic and vibrational spectroscopy). Examination of their properties as novel filter materials is ongoing.

Acknowledgement

References

1 S. Iijima, *Nature*, 1991, **354**, 56.
2 S. Iijima and T. Ichihashi, *Nature*, 1991, **363**, 603.
3 D. S. Bethune, C. H. Klang, M. S. de Vries, G. Gorman, R. Savory, J. Vazquez and R. Beyers, *Nature*, 1993, **363**, 605.
4 J. P. Issi, L. Langer, J. Heremans and C. H. Olk, *Carbon*, 1995, **33**, 941.
5 C. F. Cornwell and L. T. Wille, *Solid State Commun.*, 1997, **101**, 555.
6 M. S. Fuhrer, J. Nygard, L. Shih, M. Forero, Y. G. Yoon, M. S. Mazzoni, A. Zettl and P. McEuen, *Science*, 2000, **288**, 294.
7 R. Rosen, W. Simendinger, C. Debbault, H. Shimonda, L. Stoner and O. Zhou, *Appl. Phys. Lett.*, 2000, **76**, 1668.
8 B. Smith and D. Luzzi, *Chem. Phys. Lett.*, 2000, **321**, 169.
9 S. Lebedkin, P. Schweiss, B. Renker, S. Malik, F. Hennrich, M. Neumaier, C. Stoermer and M. M. Kappes, *Carbon*, 2002, **40**, 417.
10 A. Thess, R. Lee, P. Nikolaev, H. Dai, P. Petit, J. Robert, C. Xu, H. Lee, S. G. Kim, D. T. Colbert, G. Scuseria, D. Tomanek, J. E. Fischer and R. E. Smalley, *Science*, 1996, **273**, 483.
11 T. Guo, P. Nikolaev, A. Thess, D. T. Colbert and R. E. Smalley, *Chem. Phys. Lett.*, 1995, **243**, 49.
12 M. Monthioux, B. W. Smith, B. Burteaux, A. Claye, J. E. Fischer and D. E. Luzzi, *Carbon*, 2001, **39**, 1251.
13 A. G. Rinzler, J. Liu, P. Nikolaev, C. B. Huffman, F. J. Rodriguez-Macias, P. J. Boul, A. J. Lu, D. Heymann, D. T. Colbert, R. S. Lee, J. E. Fischer, A. M. Rao, P. C. Eklund and R. E. Smalley, *Appl. Phys. A: Mater. Sci. Process.*, 1998, **67**, 29.
14 W. A. de Heer, W. S. Bacsa, A. Châtelain, T. Gerfin, R. Humphrey-Baker, L. Forro and D. Ugarte, *Science*, 1995, **268**, 845.
15 T. Pichler, M. Knupfer, M. S. Golden, J. Fink, A. Rinzler and R. E. Smalley, *Phys. Rev. Lett.*, 1998, **80**, 4729.
16 D. A. Walters, M. J. Casavant, X. C. Qin, C. B. Huffman, P. J. Boul, L. M. Ericson, E. H. Haroz, M. J. O'Connell, K. Smith, D. T. Colbert and R. E. Smalley, *Chem. Phys. Lett.*, 2001, **338**, 14.
17 H. Rösner, S. Lebedkin, F. Hennrich, J. Tracy, A. Malik and M. M. Kappes, to be published.
18 J. Liu, A. G. Rinzler, H. Dai, J. H. Hafner, R. K. Bradley, P. J. Boul, A. Lu, T. Iverson, K. Shelimov, C. B. Huffman, F. Rodriguez-Macias, Y.-S. Shon, T. R. Lee, D. T. Colbert and R. E. Smalley, *Science*, 1998, **280**, 1253.
19 J. Chen, M. A. Hamon, H. Hu, Y. Chen, A. M. Rao, P. C. Eklund and R. C. Haddon, *Science*, 1998, **282**, 95.
20 M. A. Hamon, H. Hu, P. Bhowmik, S. Niyogi, B. Zhao, M. E. Itkis and R. C. Haddon, *Chem. Phys. Lett.*, 2001, **347**, 8.
21 M. A. Hamon, J. Chen, H. Hu, Y. Chen, M. E. Itkis, A. M. Rao, P. C. Eklund and R. C. Haddon, *Adv. Mater.*, 1999, **11**, 834.
22 J. C. Sheehan and G. P. Hess, *J. Am. Chem. Soc.*, 1955, **77**, 1067.
23 M. Holzinger, A. Hirsch, F. Hennrich and M. M. Kappes, in preparation.
24 F. Hennrich, A. Malik, H. Rösner and M. M. Kappes, in preparation.
25 *Science of Fullerenes and Carbon Nanotubes*, ed. M. S. Dresselhaus, G. Dresselhaus and P. C. Eklund, Academic Press, San Diego, California, 1996.
26 D. B. Mawhinney, V. Naumenko, A. Kuznetsova, J. T. Yates, J. Liu and R. E. Smalley, *Chem. Phys. Lett.*, 2000, **324**, 213.
27 H. Hu, P. Bhowmik, B. Zhao, M. A. Hamon, M. E. Itkis and R. C. Haddon, *Chem. Phys. Lett.*, 2001, **345**, 25.